Chitin-based double-network hydrogel as potential superficial soft tissue repairing materials

Junchao Huang, [a] Martin Frauenlob, [a] Yuki Shibata, [a] Lei Wang, [b, c] Tasuku Nakajima, [a, c, d] Takayuki Nonoyama, [a, c] Masumi Tsuda, [b, c, d] Shinya Tanaka, [b, c, d] Takayuki Kurokawa, [a, c] Jian Ping Gong [a, c, d,*]

[a] *Laboratory of Soft and Wet Matter, Faculty of Advanced Life Science, Hokkaido University, Sapporo 060-0810, Japan.*

[b] *Department of Cancer Pathology, Faculty of Medicine, Hokkaido University, Sapporo 060-8638, Japan.*

[c] *Global Station for Soft Matter, Global Institution for Collaborative Research and Education (GI-CoRE), Hokkaido University, Sapporo 001-0021, Japan.*

[d] *Institute for Chemical Reaction Design and Discovery (WPI-ICReDD), Hokkaido University, Sapporo 001-0021, Japan.*

* Corresponding authors at: Faculty of Advanced Life Science, Hokkaido University, Sapporo 060-0810, Japan. E-mail: gong@sci.hokudai.ac.jp (Jian Ping Gong).

Keywords

Chitin, double-network hydrogel, modulus, strength, toughness, tissue repairing materials

Abstract

Chitin is a biopolymer which has been proved to be a candidate as biomedical materials, yet the weak mechanical properties limited their potentials seriously. In this work, a chitin-based double-network (DN) hydrogel was designed as a potential superficial repairing material. The hydrogel was synthesized through double-network (DN) strategy composing hybrid regenerated chitin nanofibers (RCNs)-poly (ethylene glycol diglycidyl ether) (PEGDE) as the first network and polyacrylamide (PAAm) as the second network. The hybrid RCNs-PEGDE/PAAm DN hydrogel was strong and tough, possessing Young's modulus (elasticity) E 0.097 ± 0.020 MPa, fracture stress σ_f 0.449 ± 0.025 MPa, and work of fracture W_f 5.75 ± 0.35 MJ·m^{-3}. The obtained DN hydrogel was strong enough for surgical requirements in the usage of soft tissue scaffolds. In addition, the chitin endowed the DN hydrogel with good bacteria resistance and accelerated fibroblast proliferation, which NIH3T3 cell number increased nearly 5 times within 3 days. Subcutaneous implantation studies showed that the DN hydrogel did not induce inflammation after 4 weeks, suggesting a good biosafety *in vivo*. These results indicated that the hybrid RCNs-PEGDE/PAAm DN hydrogel had great prospect as rapid soft tissue repairing materials.

Introduction

Superficial soft tissue damage is one of the most common physical injuries in our normal lives, such as skin damage, *e.g.* burns, scratch, strikes and skin ulcers, and even superficial muscle

damage, *e.g.* cuts and tears. A major therapy is covering the wounds with wound dressings. Gauze and non-woven blends are known as the most frequently utilized *in vitro* dressings to facilitate wound healing. However, such dry dressings allows wound desiccate rather quickly which induces strong pains and microbial invasion, also the adhesion and even bonding to the wound surface lead to difficulties of removing, or the second time damage when removing the dressing, which is confronted with a great challenge in wound caring.[1-3] In the case of muscle damages, such as muscle cuts and tears, not only the repair surgery is necessary, sometimes the suitable scaffolds are used at the same time to support the tissue and promote the wound healing. Yet the development of high mechanical strength scaffolds is a great challenge.

Natural polymers have been widely used as biomedical materials owing to their biophysical similarity to soft biological tissues.[4, 5] Because of the excellent hydrophilicity, biocompatibility and biodegradability, the hydrogels constructed by cellulose[6], alginate[7], collagen[8], dextran[9], silk[10] and hyaluronan[11] are regularly considered as candidates for artificial tissue, scaffolds and extracellular matrix. But the poor bacterial barrier capacity restricts the direct applications except for embedding with antibiotics, metal ions or nanoparticles[12-15], which also brings in possible inflammation and allergy *in vivo*[16, 17]. Natural polymer extracted from marine crustaceans and fungi, so-called chitin and its derivatives, chitosan, which has also been proved to accelerate fibroblast proliferation, are regarded as more promising matrix as wound repairing materials[18, 19]. At the early study, the chitin-based repairing materials were mainly designed as wound dressings, which were based on chitin nanofibers, whiskers, nanocomposites, *etc*[20-22]. Current researches on chitin-based hydrogels used for wound repairing are focus on the blending and co-spinning with other synthetic polymers for enhancing strength and flexibility, such as PVA, PEG and PVP and other natural polymers such as collagen, cellulose, chitosan and their derivates[18, 22]. But the poor

mechanical strength and low moisture retention capacity of these chitin-based materials are still dissatisfied as required. The drawbacks are originated from insufficient processing method due to the great resistance against most of solvents of chitin.

Precious studies have demonstrated the relationship between the elasticity of the substrate and the cell phenotype. Discher *et al.* hypothesized that cells maybe mechanosensitive to the substrate stiffness.[23] Specifically, a relative high modulus is essential for activation, differentiation and proliferation of fibroblast and myoblast phenotype[24-27], which is important in the myoideum healing. Therefore, in the fabrication of materials for the wound healing *in vivo*, the elasticity of the materials should be considered. The presented chitin-based hydrogels for *in vivo* treatments are generally designed as the injectable thermosensitive hydrogels, which is easy handling and can fill the defect area of the wounds to minimize the invasive surgical procedures. In the case of the cells culturing in a three-dimensional extracellular matrix, the easy mixing of cells and injectable hydrogels promotes cell growth significantly partially owing to a wide area of contact.[28-30] However, the injectable chitin hydrogels generally have a relatively low elasticity (5 ~ 20 kPa) and may limit fibroblast phenotype in the case without cytokines.[24, 26] Hence chitin materials with high elasticity are required for fibroblast proliferation.

Recent studies on the native chitin nanofiber-based films and membranes have drawn attentions due to its high mechanical strength. The native chitin nanofibers are generally produced through simple mechanical and chemical treatments which are able to remain a high aspect (length/diameter) ratio.[31] As a result, the self-assembled materials made from these native chitin nanofibers, such as nano-film, nano-paper and nano-sheet, have excellent mechanical properties.[32-34] However, the native chitin nanofiber dispersion to prepare film and membrane is always of low

concentration and requires water evaporation during preparation, the resulting dry and very thin films and membranes maybe highly restricted in the usage as wound healing materials. Besides, the redispersion of the nanofibers in water may occur without crosslinking which limits its applications as wound healing materials *in vivo*. Injectable hydrogels based on native chitin nanofibers used as the extracellular matrix are also rarely seen.[35] Compared to the native chitin nanofibers, the applications of regenerated chitin nanofibers (RCNs) have a wider outreach, which can be produced by dissolving chitin in a suitable solvent then regenerating it from the solvent by solvent exchange[36]. So far, several solvent systems are used for chitin dissolution, which produces RCNs and its materials, including hexafluoro-2-propanol (HFIP), lithium chloride (LiCl)/*N*, *N*-dimethylacetamide (DMAc) composite solvent, sodium hydroxide (NaOH)/urea aqueous solution and potassium hydroxide (KOH)/urea aqueous solution[37-42]. The RCNs based hydrogels is able to hold a large amount of water, but at the same time, they are weak and brittle.

To overcome the current mechanical weakness of chitin hydrogels, the double-network strategy is an efficient method to develop chitin-based tough hydrogels[43]. A double network hydrogel (DN hydrogel) consists of two interpenetrated networks with contrasting structure: the first network is rigid and brittle, and the second network is soft and stretchable[44]. Also, another important factor to create a DN hydrogel is that the first network gets swell largely in the second network monomer solution.[45] The low aspect ratio of RCNs leads to the network brittleness and weakness[46], which can fulfill the mechanical strength requirement as the first network in the double-network strategy. However, due to the strong aggregation tendency, the chitin nanofibers in the dispersion self-assembles to a physical hydrogel with dense structure during the preparation of RCNs, which is unable to swell largely in neither water nor the hydrophilic monomer solution. Hence the second

network formed in a physical RCNs based hydrogel is unable to exert the double network effect, resulting in poor mechanical properties.

A common method to construct a highly swollen RCNs based network is introducing epoxy chemicals as crosslinker into the chitin dispersion.[47-49] The chitin dispersion was prepared by using aqueous KOH/urea solution as previously reported.[50] Different from synthetic polymers, the concentration of the epoxy crosslinker largely excess the molar ratio of monomer units of chitin. The epoxy crosslinker not only consumes all hydroxyl groups on RCNs, but also self-react to form another network. As a result, the RCNs-based hydrogel prepared by this method is a hybrid network which is composed of nanofibers-*g*-crosslinker network and crosslinker-*g*-crosslinker network. After reacted with EGDE then washed by water, the RCNs based hydrogel is achieved. Owing to the flexible crosslinker-*g*-crosslinker network, the hydrogel swells largely in water and hydrophilic monomer solution, which is suitable for being reinforced by double-network strategy. A simple and biosafe polyacrylamide is also selected as the second network in this work to fabricate a tough RCNs-based/polyacrylamide double-network hydrogel. Combining with the rapid fibroblast proliferation ability and good bacteria resistance of chitin, the enhancement in mechanical properties of the DN hydrogel has great prospects as the wound repairing materials, such as hydrogel wound dressing and superficial soft tissue scaffolds. Introducing epoxy crosslinker is one of the regular methods to prepare chitin and other natural polymer hydrogel, however, the attempting to prepare DN hydrogel by a hybrid network in this work is rare. The co-construction of stiff nanofibers and soft network for highly swelling hydrogel preparation will inspire another strategy to construct natural polymer based DN hydrogel with high toughness.

Experimental section

Materials and reagents. The raw squid pens extracted from *Todarodes pacificus* were purchased from Kaneshime Takahashi Suisan (Hokkaido, Japan). As the raw squid pen contained mainly chitin and minor protein and minerals, before usages, raw squid pens were subsequently demineralized and deproteinized twice by 4% (w/v) hydrochloric acid and 4% (w/w) sodium hydroxide solution, respectively. The treated squid pens were washed by deionized water at each step and then freeze-dried to obtain purified *β*-chitin. The molecular weight of purified *β*-chitin was determined as 1.2 - 2.0 × 10^6 g/mol at 5% LiCl/95% DMAc (w/w) and 25°C by size exclusion chromatography[51], and the degree of acetylation was determined as 98.7% by two abrupt change conductometric titrations[52]. Acrylamide (AAm), ethylene glycol diglycidyl ether (EGDE), *N*, *N'*-methylenebisacrylamide (MBA), and 2-oxoglutaric acid (α-keto) were purchased from Fujifilm Wako Pure Chemical Industries (Japan) and used without any pretreatments.

Luria-Bertani broth (LB) and agar were obtained from Fujifilm Wako Pure Chemical Industries (Japan). Gram-positive bacteria *Micrococcus luteus* (*M. luteus* NBRC 3333) and Gram-negative bacteria *Escherichia coli* (*E. coli* strain K-12) were employed in the antibacterial test. Dulbecco's modified Eagle's medium (DMEM) was purchased from Nissui Pharmaceutical (Tokyo, Japan); penicillin-streptomycin, trypsin-EDTA, and HEPES were from Sigma-Aldrich (St. Louis, MO, USA); and fetal bovine serum (FBS) was from Gibco®-life Technologies (Grand Island, NY, USA). The murine embryonic fibroblasts (NIH3T3) were purchased from JCRB (Japan). Calcein-AM, (sodium 2, 3-bis(2-methoxy-4-nitro-5-sulfophenyl)-5-[(phenylamino)-carbonyl]-2H-tetrazolium) inner salt (XTT), (*N*-methyl dibenzopyrazine methyl sulfate) (PMS) and propidium

iodide (PI) were purchased from Wako Pure Chemical Industries (Japan). The live/dead bacteria kit (SYTO9/PI) was purchased from Invitrogen (Thermo Fisher Scientific).

Preparation of RCNs-PEGDE hydrogel. A 2 g of the purified *β*-chitin was suspended in 98 g of aqueous KOH/urea solution containing 20 g KOH and 4 g urea, and then dissolved by freezing-thawing method[53]. A 7.7 mL of EGDE as chemical crosslinker was added and then vigorously stirred to mix them well. The mixed solution was degassed, and subsequently stored for 4 h at 15°C to form stable as-prepared gel. The as-prepared gel was totally washed by deionized water to get the highly swollen first network hydrogel namely RCNs-PEGDE hydrogel. The initial concentration of chitin (c_{chitin}^{i}) was 24.1 g/L and the molar concentration of EGDE relative to chitin monomer (c_{EGDE}) was 500 mol%. For convenience, the RCNs-PEGDE hydrogel was coded as SN in the following text.

Preparation of RCNs-PEGDE/PAAm double-network hydrogel. The SN hydrogel was immersed into 3mol/L AAm solution containing MBA (crosslinker) and α-keto (initiator) for 1 d. The concentration of MBA and α-keto were both 0.02 mol% relative to AAm monomer. After highly swelled in AAm solution, the precursor chitin gel was sandwiched between two hydrophobic sheets and glass plates, and the system was lightly pressurized to expel access AAm solution on the surface. The polymerization of AAm was performed using 365 nm UV light irradiation (4 mW/cm^2) for 8 h under argon atmosphere. After polymerization, the sample was further fully washed and swelled in deionized water. The sample thus achieved was chitin-PEGDE/PAAm double-network (DN) hydrogel. For convenience, the chitin-PEGDE/PAAm DN hydrogel was coded as DN in the following text.

Attenuated total reflectance Fourier-transform infrared spectroscopy (ATR-FTIR). The ATR-FTIR measurements on β-chitin and SN hydrogel were performed by a FT-IR 6600 spectrometer (JASCO, Japan) with diamond prism. The applied β-chitin sample was ungrounded purified squid pen, and the SN hydrogel was cut into dish-like shape with a thickness of 0.5 mm. The spectra were measured in full contact with the prism for wavenumbers of 4000 - 700 cm^{-1}, at 32 times accumulation and at a resolution of 2 cm^{-1}. The air background was subtracted by the accessory software.

Water content measurements. The water content of all sample hydrogels swollen in pure water was measured using the moisture balance (Moisture Balance; MOC-120H, Shimadzu Co., Japan). Water inside the hydrogel was gradually evaporated from 30 to 120°C until no longer changed. The water content (ω, %) was calculated as the ratio percentage between the weight of water in hydrogel to the total weight of the hydrogel. The results were average of three specimens.

Swelling ratio measurements. The as-prepared SN gel was chosen as the reference state. The swelling ratio was defined as $Q_v = V_{sw}/V_{as}$, where V_{sw} was the volume of fully swollen SN or DN hydrogel and V_{as} was the volume of as-prepared SN gel. The volume of the gel was measured through its three-dimension length. The true chitin concentration ${c_{chitin}}^t$ in SN and DN hydrogel was calculated as ${c_{chitin}}^t = {c_{chitin}}^i/{Q_v}^{SN}$ and ${c_{chitin}}^t = {c_{chitin}}^i/{Q_v}^{DN}$, respectively.

Tensile test. The tensile test was performed on a universal testing system (Instron 5965, US) at a stretch velocity 100 mm/min. The samples were cut into dog bone shape with 100.0 mm length and 10.0 mm width. The fracture stress σ_f and strain ε_f were both directly obtained from the nominal stress and stress at the fracture point. The Young's modulus E was calculated as the slope of the initial stress-strain curve. The work of fracture W_f was calculated from the area under the stress-

194 strain curve. The values of all the mechanical properties were calculated as averages for at least
195 five specimens. All measurement was performed at the temperature of 25°C and in water vapor
196 environment to avoid sample drying.

197 **Bacteria killing kinetics test.** This test was used to study the bacterial killing kinetics on the
198 PAAm, SN and DN hydrogels. Briefly, *M. luteus* and *E. coli* were allowed to grow in LB broth to
199 reach a concentration of 2.5×10^7 CFU/mL. Thereafter, 10 mL of bacteria suspension was
200 centrifuged (4,500 rpm, 8 min) to remove supernatant, and then re-suspended in 1 mL saline. At
201 the same time, 5 μL live/dead backlight bacterial viability kit (SYTO9/PI, Invitrogen) was added
202 into the above bacteria/saline suspension. Then 2 μL of the suspension was spread on the hydrogel
203 surface with plastic razor blade. The agar was used as a control. All samples were immersed into
204 saline for 1 d before this test. The samples with bacteria were placed and observed by a fluorescent
205 microscope with time-lapse system (Eclipse Ti-E Inverted Microscope, Nikon Instruments Inc.,
206 Japan). SYTO9 is a dye that stains living bacteria which fluoresces in green (*Ex.*: 485 nm, *Em.*:
207 498 nm). PI dye stains only dead bacteria and fluoresces in red (*Ex.*: 535 nm, *Em.*: 617 nm). The
208 interval for each snapshot was set as 15 min and the total time was 18 - 20 h. An environment
209 system was used and adjusted to optimal temperature and relative humidity (R.H.) for *M. luteus*
210 (30^oC, 100% R.H.) and *E. coli* (37^oC, 100% R.H.). The survival rate of bacteria was defined as the
211 ratio of live and total bacteria counting. The experiment was repeated three time to get average
212 result.

213 **Bacterial inhibitory test.** The bacteria inhibition rate was measured to characterize the efficacy
214 of the hydrogel samples against bacteria. The bacteria were allowed to grow in the LB broth to
215 reach a concentration of 2.5×10^7 CFU/mL. Then 2 μL suspension was spread on surface of

hydrogel samples and then incubated at 30°C (for *M. luteus*) and 37°C (for *E. coli*) with shaking at 150 rpm for 24 h. All hydrogel samples were cut into a dish-like slices with diameter and thickness of 2 cm and 2 mm, respectively. The samples were immersed into LB broth for 1 d before the test. The agar was used as a blank control. After incubation, the hydrogel samples with bacteria were washed by 1 mL saline for three times to enrich all bacteria. After centrifuging at 4,500 rpm for 8 min, the supernatant was removed, and the bacterial were re-suspended with 1 mL saline. To calculate the concentration of the bacteria suspension, the absorbance at 625 nm (OD_{625}) was measured by UV-Vis spectrophotometer (UV-1800, SHIMADZU, Japan). The experiments were performed three times to get average. The inhibition rate was defined as the growth reduction of bacteria on hydrogel and agar, which was calculated as followed:[54]

$$\text{Inhibition rate}, \% = 100 - \frac{OD_{625}(\text{on hydrogel}) - OD_{625}(\text{initial inoculum})}{OD_{625}(\text{on agar}) - OD_{625}(\text{initial inoculum})} \times 100$$

Cell morphology observation. The murine embryonic fibroblasts (NIH3T3) were cultured in DMEM supplemented with 10% FBS, 1% penicillin-streptomycin and 1% L-glutamine in a humidified 5% CO_2 atmosphere. The cells were seeded into a 12-well tissue culture plate at a density of 5×10^4 cells/well and incubated in 1 mL of DMEM for 4 h for immobilization. Then, the DMEM was removed and gently settled the PAAm, SN and DN hydrogel samples on the top of cell layer. After that, 0.5 mL of fresh DMEM was added into each well and then incubated for 24 h. All hydrogel samples were sterilized in HEPES buffer and immersed into DMEM for 1 d before this experiment. The blank control was performed without any hydrogels. After 24 h, the DMEM and hydrogel samples were gently removed, further 1 mL of DMEM with Calcein-AM/PI dye was added into each well and incubated in the dark for 30 min to stain all cells. The stained cells were observed under fluorescent microscope.

Cell viability assay. The NIH3T3 cell suspension at a density of 2×10^5 cells/well was added into 12-well plate with the PAAm, SN and DN hydrogel samples and incubated for 24 h. After that, 0.5 mL of trypsin-EDTA was added into each well for 60 s, and all the cell were harvested by 4.5 mL DMEM. After replacement by fresh DMEM, 20 μL of cell suspension was mixed with 20 μL of 0.4% trypan blue and counted the blue dead cells under microscope. The cell viability was calculated by the ratio of the dead cell and total cell counting. All hydrogel samples were sterilized in HEPEs and immersed into DMEM for 1 d before this experiment. The blank petri dish was used as a control.

Cell proliferation measurement. To measure the cell number quantificationally, an XTT assay was employed. The XTT immerses into cell and reduces to an orange, water-soluble formazan products. Before the experiment, a standard curve of absorbance versus cell concentration was built to estimate cell number linear area and detection limitation (see Supporting Information **Figure S5**). The NIH3T3 were cultured in DMEM supplemented with 10% FBS, 1% penicillin-streptomycin and 1% L-glutamine in a humidified 5% CO_2 atmosphere. The cells were seeded into a 12-well tissue culture plate at a density of 2×10^5 cells/well and incubated in 1 mL of DMEM for 4 h for immobilization. Then, the DMEM was removed and the PAAm, SN and DN hydrogel samples with thickness of about 1 mm and diameter of 2 cm were gently settled on the top of cell layer in triplicate. To make sure the cells grew consecutively, the hydrogel samples were divided into 7 groups and only 1 group of samples was used for daily measurement. After the hydrogel placement, new DMEM was added into each well. The volume of DMEM was controlled to cover all the cells and avoid the floatage of hydrogel samples. The DMEM was exchanged each three days. At each daily measurement, the DMEM was gently removed. The cells and hydrogel samples were treated with 200 μL trypsin-EDTA twice and harvested into 1 mL DMEM. The well plate

and hydrogel samples were carefully washed by 1 mL DMEM to ensure all cells were harvested and mixed with the trypsin-EDTA treated one. After centrifugation, the supernatant was removed, and the cells were resuspended in 200 μL DMEM. After that, 100 μL of cell suspension with 20 μL XTT (supplemented by 2% PMS) was incubated for 4 h (counted into the total incubation time). The other 100 μL of cell suspension was used as reference. After 4 h, the absorbance values of each cell suspension were measured in triplicate at the wavelength of 450 nm and 655 nm. The absorbance of cell suspension was calculated as A_{450nm} - A_{655nm} and the resultant absorbance of formazan was calculated as A_{test} - $A_{reference}$. The cell number after daily proliferation was calculated according to the standard curve. The experiment was repeated for three times to get average.

Histopathological study. Wound histology specimens were performed under the dorsal skin of rabbits. The rabbits were mature female Japanese white rabbits which were weighed 3.9 kg in average. Before surgery, the fur on rabbit dorsum was shaved off and each rabbit was anesthetized by isoflurane. Three rectangular sterilized hydrogel samples were implanted among the connective tissue through an incision surgery, and surgical suture was also employed for hydrogel immobilization. After surgery, the rabbits were allowed to move and have solid rations and water freely in their cages. The histopathological slices were made from the tissues contacted with hydrogel and collected on day 7, 14 and 28. All the specimens were fixed in 4% paraformaldehyde solution for 2-3 days. The samples were embedded in paraffin, and 3 - 4-μm-thick tissue sections were prepared. Representative sections were stained with hematoxylin and eosin (H&E) for observation by light microscopy. For the control groups, an incision was made at the same position on another rabbit and the injured tissue sections without hydrogel contact were used for histopathology study. Three rabbits were used in each group. After the experiments, all rabbits

were euthanized. The animal studies were performed in accordance with the protocol approved by the Institutional Animal Care and Use Committee at Hokkaido University Faculty of Medicine.

Result and discussion

Figure 1a showed the preparation process of the highly swollen first network combined with chitin and EGDE. Herein, the chitin resource is extracted from squid pen and namely *β*-chitin[55], it was purified and dissolved in an aqueous KOH/urea solution by freezing-thawing cycle.[50, 53] Due to the strong inter- and intramolecular hydrogen bonding, the chitin molecules tended to aggregate into nanofibers even in a strong polarity solvent which chitin solution was a dispersion consisted of chitin nanofibers, as shown in Figure 1a. Distinguished from the polymerization of traditional poly-(2-acrylamido-2-methyl-1-propanesulfonic acid) (PAMPS) first network[43], the first network was prepared through a typical sol-gel method by employing a water-soluble crosslinker EGDE, which reacted with the exposed hydroxyl groups on the surface of chitin nanofibers, as shown in Figure 1b. After reacted with EGDE and washed by deionized water, the chitin nanofibers regenerated from the dispersion and became insoluble and formed RCNs based hydrogel. The FTIR result showed that the intensity of -CH_2- and -OH group significantly increased after reaction, suggesting the formation of RCNs-PEGDE networks (see Supporting Information **Figure S1**). Notably, the molar mass of EGDE was well in excess to that of chitin monomer, suggesting after the hydroxyl groups on the surface of nanofibers were consumed, the residual EGDE continued to form PEGDE homo-polymer (Figure 1c), and created a hybrid first network which was combined with RCNs-PEGDE and PEGDE-PEGDE network. However, it was no way to form a pure PEGDE gel under the same EGDE concentration applied in the chitin dispersion. After reaction, the as-prepared first network was washed by large amount of deionized water and got

swelled during the washing, which volume swelling ratio Q_v of the gel reached to about 5.4 in relative to the as-prepared chitin gel. Furtherly, the first hybrid network was immersed into AAm solutions containing initiator and crosslinker for further swelling, then the PAAm second network was synthesized in the presence of the first network under UV light to get as-prepared DN gel. After the as-prepared gel was washed and swelled in deionized water (Q_v ~ 9.0, in relative to the as-prepared first network gel, **Table 1**), the DN hydrogel was achieved.

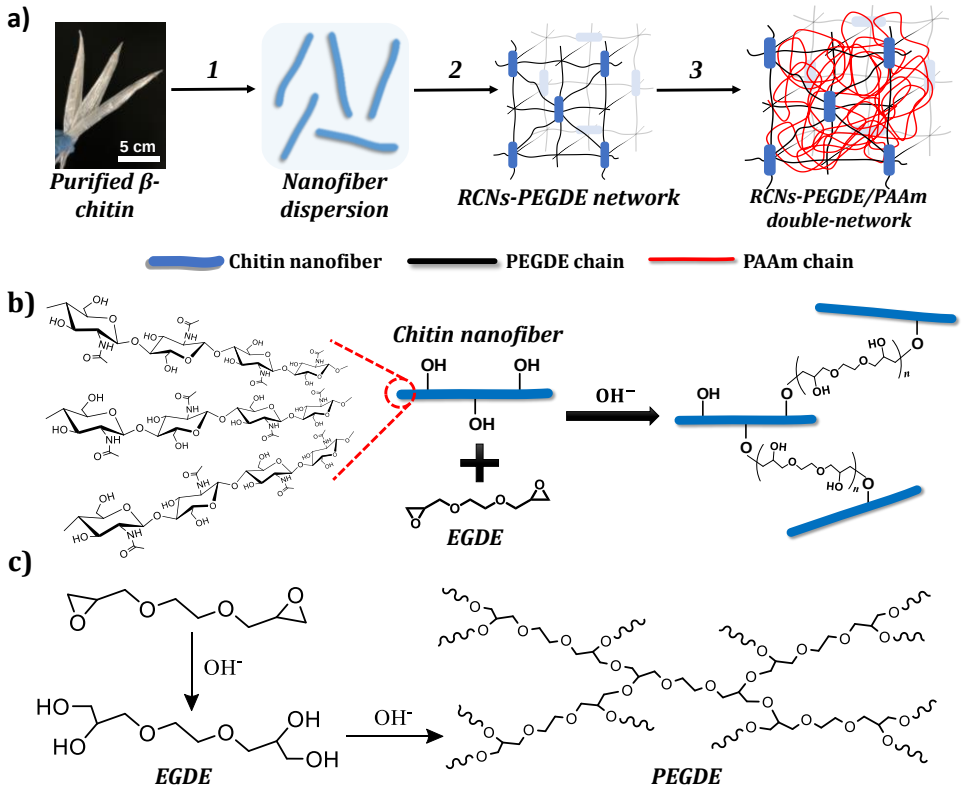

Figure 1. (a) Illustration of the preparation process of the RCNs-PEGDE hydrogel (SN hydrogel) and the RCNs-PEGDE/PAAm DN hydrogel (DN hydrogel): (1) The *β*-chitin was dissolved in aqueous KOH/urea solution to form a chitin nanofiber dispersion; (2) A desired amount of EGDE was added into the dispersion to react with chitin nanofibers or themselves to form a hybrid network, and after washing and swelling in DI water, the first network was obtained; (3) The

second PAAm network was synthesized under UV light and argon atmosphere, and after washing and further swelling in DI water, the DN hydrogel was obtained. **(b)** Reaction between RCNs and EGDE. Each RCNs was composed of several chitin molecules which were aggregated through hydrogen bonding. Only the hydroxyl groups exposure on the surface of RCNs were able to react with single or multiple EGDE molecules under alkali condition and formed covalent bonds. **(c)** Self-reaction of EGDE molecules under alkali condition. The wavy line referred to crosslinking with other EGDE.

Table 1. Formulation of SN and DN hydrogels, volume swelling ratio (Q_v) in relative to the as-prepared chitin gel and water content (ω, %) of SN and DN hydrogels in pure water, and true chitin concentration (c_{chitin}^t) calculated through Q_v in the hydrogels.

Sample	1st network	2nd network	Q_v	ω, %	c_{chitin}^t, g/L	E, kPa
SN hydrogel	2.0 wt% chitin, 500 mol% *EGDE*	-	5.4	98.4	4.5	6.8 ± 0.9
DN hydrogel	2.0 wt% chitin, 500 mol% *EGDE*	3 M AAm, 0.02 mol% MBA, 0.02 mol% α-keto	9.0	89.3	2.7	97 ± 20

Figure 2 showed the photograph (a) and mechanical strength (b-d) of the chitin-PEGDE SN and DN hydrogels. The transparent SN hydrogel containing more than 98% water was very brittle and it broke even by a bending deformation (Figure 2a). From the swelling ratio Q_v of SN hydrogel, the true chitin concentration c_{chitin}^t in SN hydrogel was calculated as 4.5 g/L, as shown in Table 1. After being reinforced by PAAm through DN strategy, the DN hydrogel became tough enough

that sustained a large deformation. The fracture stress σ_f, fracture strain ε_f and Young's modulus E values of the SN hydrogel were only 4.5 ± 1.2 kPa, 0.5 ± 0.1, 6.8 ± 0.9 kPa, respectively, and those of PAAm hydrogel were 64 ± 6.3 kPa, 13.6 ± 2.1, 12.1 ± 2.9 kPa, respectively (Figure 2b). The mechanical strength of the DN hydrogel was much higher than the SN and PAAm hydrogel, showing a stress-strain curve similar to that of previously reported tough PAMPS/PAAm DN hydrogel with yielding behavior[56], as shown in Figure 2b. DN hydrogel had a significant high W_f of 5.75 ± 0.35 MJ·m^{-3}, and σ_f, ε_f and E values were 0.449 ± 0.025 MPa, 14.0 ± 2.4 and 0.097 ± 0.020 MPa, respectively (Figure 2b). σ_f of the DN hydrogel was of almost 100 times to that of than the SN hydrogel. However, the water content of the DN hydrogel slightly reduced to 89%, which meant that the PAAm network was restricted to swell by the SN network. From the swelling ratio Q_v of the DN hydrogel, the total polymer content in DN hydrogel was estimated about 130 g/L while the $c_{chitin}{}^t$ in DN hydrogel decreased to 2.7 g/L due to swelling of SN hydrogel in AAm solution and the further swelling of the as-prepared DN hydrogel in water (Table 1). Compared to the other chitin-based blended hydrogels, chitin nanocrystals/PAAm[57], chitin whisker/alginate composite hydrogel[58], chitin/PVA hydrogel[47], nanoparticle reinforced chitin hydrogel[48, 59, 60], double-crosslinked chitin hydrogel[61], and the native chitin nanofiber-based hydrogels[62-66], the RCNs-PEGDE/PAAm DN hydrogel developed in this work was tougher (larger W_f) and stronger (larger σ_f), which was able to undergo suture surgery. Also, the high modulus of the DN hydrogel should favor the requirement for fibroblast activation and proliferation as previously reported.[26, 67] In this work, the toughening strategy for the SN hydrogel referenced the pre-stretching strategy that had applied to the neutral polymer-based first network[45, 68], through introducing an additional flexible component to improve the network stretchability to obtain a higher swelling ratio for the fabrication of tough DN hydrogel. In various physiological saline and PBS buffer solutions, as

well as in various pH solutions, the DN hydrogel deswelled very slightly (**Table S1**), which might be owing to the high osmotic pressure of the concentrated neutral PAAm in the DN hydrogels. The slight deswelling lead to small changes on mechanical properties under various media (Figure 2c and 2d), but it remained the similar mechanical strength, indicating a good stability in physiological fluids.

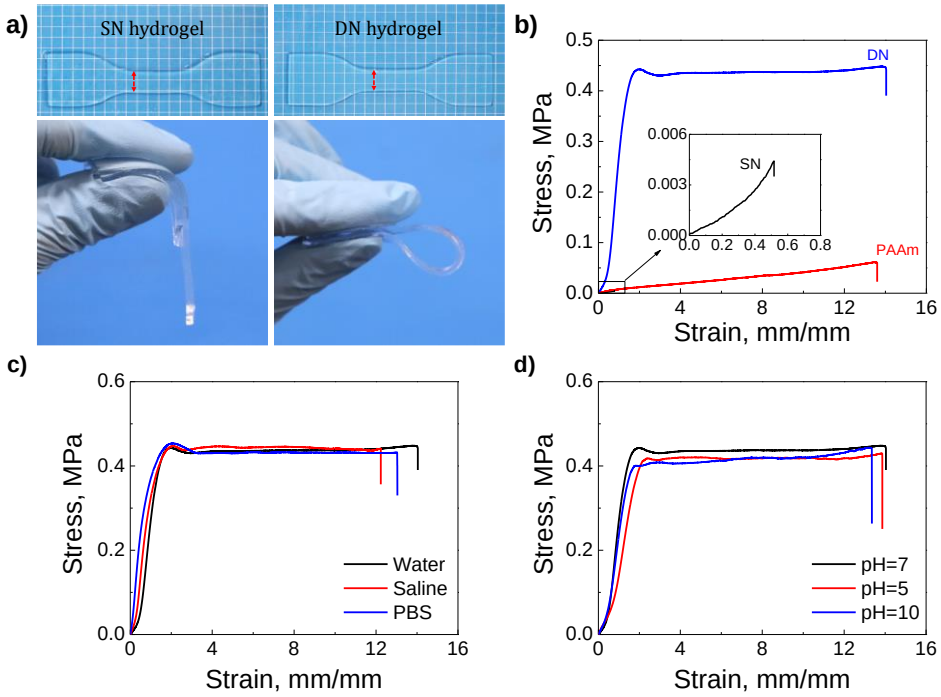

Figure 2. (a) Photography of the chitin-PEGDE SN hydrogel and the DN hydrogel. The lattice length in (a) was 5 mm. Upper photos: samples in dog bone shape for tensile test; lower photos: SN hydrogel broken after bending (left) while DN hydrogel allowed bending (right). (b) Tensile stress-strain curves of the SN hydrogel, PAAm hydrogel, and the DN hydrogel swollen in water. (c, d) Tensile stress-strain curves of the DN hydrogel after equilibrium in different buffers (c) and solutions with different pH values (d).

One of the essential properties as wound dressings is the strong resistance to bacterial infection. Chitin and chitosan have excellent antibacterial ability due to the potential to have protonated amino and acetylamino groups, and the antibacterial ability increases with content of amino groups.[69] Herein, the degree of deacetylation (*D.D.*) of chitin hydrogel was determined as 5.9% due to possible deacetylation in alkali solution during dissolving. The M_w of chitin might decrease due to the alkali degradation, but the decrease was reported to be small after dissolution and would not change the physiochemical properties apparently.[70] Generally, the antibacterial ability was confirmed by the bacteriostatic (bacteria-inhibiting) and bactericidal (bacteria-killing) tests.[71] **Figure 3a** and 3b showed the inhibition rate and survival rate of the PAAm, SN and DN hydrogel against *E. coli* (Gram-negative) and *M. luteus* (Gram-positive), respectively. The inhibition rate demonstrated the bacteriostatic capacity of the hydrogel and it was calculated according to the bacteria colony-forming unit changes after incubation on agar and other samples. Agar had no inhibition or killing effect against bacteria and was used as blank control. To measure the inhibition rate, *E. coli* and *M. luteus* were spread on the PAAm, SN and DN hydrogel in the presence of culture medium and allowed to grow under their optimal growth temperature. After incubation for 24 h, all bacteria on the hydrogel was harvested and the concentration was measured by spectrometer method to quantify the inhibition rate. The inhibition rate of the hydrogel sample was around 75% - 90% against *E. coli* and 50% - 75% against *M. luteus*, respectively (Figure 3a), showing a favorable resistance against bacteria growth. The survival rate demonstrated the bactericidal capacity of the hydrogel and it was calculated according to the live/dead bacteria ratio after incubation on agar and other samples. A bacterium killing kinetics experiment was firstly performed on the SN hydrogel to determine the time range. As shown in **Figure S2** and **Movie S1**, the bacteria gradually died (turned green to red) and the survival rate decreased with incubation

time and reached to a constant after 12 h which confirmed the end of bacteria killing. Hence the time range of killing kinetic measurements for other samples were based on 12 h for comparation. On the agar one, about 25% of *E. coli* and 35% of *M. luteus* were dead after 12 h incubation due to possible dehydration. For the PAAm sample, the survival rate was similar to that of agar, which showed no bactericidal capacity against *E. coli* and *M. luteus*. This was because the amino groups on polyacrylamide were difficult to be protonated, which result in a lack of antibacterial ability. While on the SN hydrogel, only 14% of *E. coli* and 7.5% of *M. luteus* survived after 12 h incubation, indicating a good bactericidal capacity. On the DN hydrogel, most of the bacteria dead after incubated for 12 h, as shown in Figure 3c and 3d, and the survival rate was 27% for *E. coli* and 23% for *M. luteus*, which was higher than that on the SN hydrogel due to the low concentration of protonated amino groups on the hydrogel surface[72]. As the results showed here, it was reasonable to conclude that the DN hydrogel had good bacterial resistance. The bacteriostatic and bactericidal capacity of chitin hydrogels were originated from the electrostatic interaction between the negatively charged cell wall of bacteria and the protonated amino groups fixed on the surface of DN hydrogels[73], but because of the localized chitin molecules on the surface of DN hydrogel, there was a time gap for the bacteria to contact with the hydrogel surface and interact with chitin molecules[74]. Unlike diffusible antibiotic and chemicals with strong positive charge such as silver ions, zinc ions, chitosan oligomer and its derivatives and tetraalkylammonium salts, their strong antibacterial activity might serve in a short-term in relative to their dose level, which would be used as emergency disinfection. Compared to the above chemicals, the relative low inhibition rate and long killing time of the DN hydrogel in this work demonstrated a mild antibacterial capacity, but it also suggested the possible long-term antibacterial activity, which might be benefit in a long therapeutic procedure. Specifically, chitosan was considered as potential inflammation incentives

because the abundant amino groups might cause serious proinflammatory response when they were protonated *in vivo*[75], and as a result, the content of amino group must be controlled to minimize the possible inflammations in our cases. Without any doubt, the antibacterial capacity of chitin could be enhanced by moderately increasing positive charge through deacetylation treatment or cationic modification.

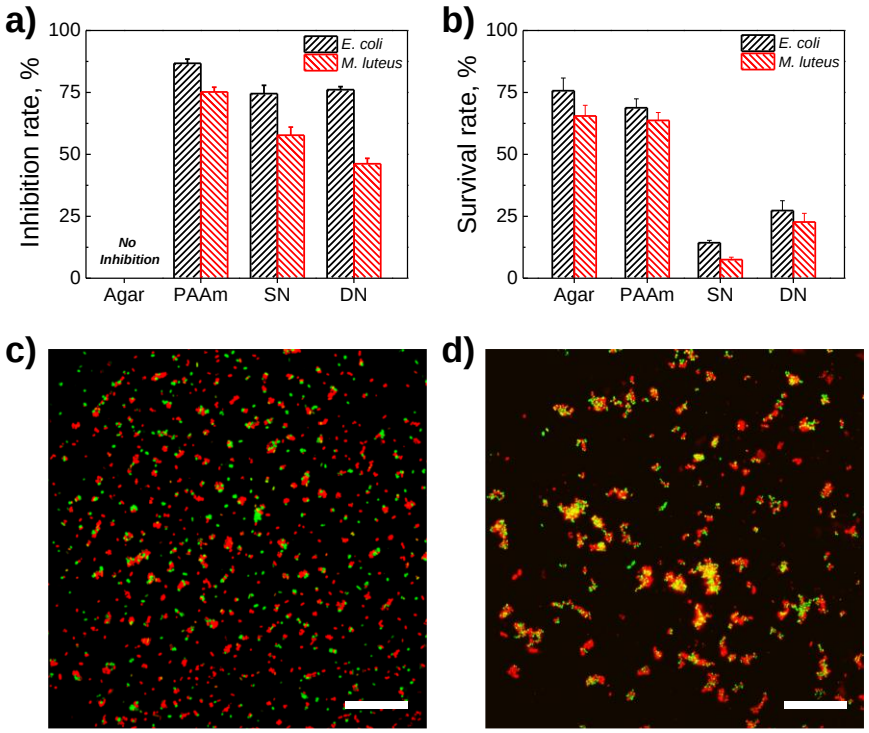

Figure 3. (a) Inhibition rate of the agar, PAAm, SN, and DN hydrogel samples against *E. coli* and *M.luteus*. (b) Survival rate of the bacteria after incubation on the samples for 12 h. Each measurement was performed in triplicate. (c, d) Fluorescent microscope images of live (green) and dead (red) *E. coli* (c) and *M. luteus* (d) after incubation on DN hydrogel for 12 h. Scale bar = 100 μm.

Differ from the transplantation materials, the wound dressing always required non-adhesion to the tissues for further painless removing. Generally, the cell adhesion on hydrogel occurred with the involvement of cell adhesion receptors and corresponding proteins, and therefore, without appropriate design, most of synthetic hydrogels, including PAAm hydrogel, were anti-adhesive[76]. Chitin was reported having effects on promoting fibroblast[77], but the cell adhesion on chitin hydrogel was weak because of the very low positive charge density[78]. As shown in **Figure S3**, NIH3T3 cells properly adhered on petri dish and grew in regular shape, while on the PAAm, SN and DN hydrogel, the NIH3T3 cells deactivated and floated, and aggregated into large bundles, suggesting that these hydrogels were non-adhesive to the cells. As a result, to minimize the cell aggregate and simulate the cell growth under the effect of hydrogels *in vitro*, the cells were seeded on the petri dish at first for immobilization then covered by hydrogels and incubated for subsequent measurements. **Figure 4a** and 4b showed NIH3T3 cell morphology and viability after incubation on the petri dish, PAAm, SN and DN hydrogel *in vitro*. The stained NIH3T3 cells grew in their regular long spindle or polygon shape on the petri dish. When the cells contacted with the PAAm, SN and DN hydrogels, the cells grew in the same shape as that on the petri dish (Figure 4a), indicating no significant inhibition by hydrogel contact. In addition, the cell viability was higher than 98% when contacted with the hydrogels (Figure 4b), also indicating the non-cell-cytotoxicity of the hydrogels. Further, to demonstrate the contact-mediated acceleration effect of the DN hydrogel on NIH3T3 cells, a daily XTT assay, which has been demonstrated to be more sensitive and harmless than MTT assay, was employed[79]. The calibration curve for XTT measurement was established at first to acquire the linear detection region, which was ranged from 2.0×10^5 to 3.0×10^7 (see Supporting Information **Figure S4a**). At day 0, the NIH3T3 cells were seeded on petri dish with a cell number of 2.0×10^5 cells/dish and then each hydrogel sample was placed upon the

cells to exert its influence. After incubation and proliferation for a time interval, the daily XTT assay was performed and the absorbance result was recorded, as shown in Figure S4b. The cell concentration versus time calculated according to the calibration curve (see Supporting Information Figure S4c) was shown in Figure 4c. The cells grew on petri dish, increased gradually from 2.0×10^5 to 3.5×10^5 cells from day 0 to day 3. Compared to that incubated on petri dish, when the cells contacted with the PAAm, SN and DN hydrogel, they grew faster and the cell number significantly increased to 6.7×10^5, 8.3×10^5 and 9.8×10^5 at day 3, respectively, which cell number showed 3.4, 4.2 and 4.9 times increase compared to day 0. According to these results, the SN and DN hydrogels showed similar promotion effect on fibroblast proliferation, although the c_{chitin}^{t} in the DN hydrogel was lower than that of the SN hydrogel. Since the previous studies have shown that that the promotion on fibroblast was effected by chitin concentration[77, 80], it was reasonable to interpret that the promotion on fibroblast proliferation was originated from the higher modulus of the DN hydrogel than the SN hydrogel (Table 1)[24, 25, 27]. The accelerated effect of the DN hydrogel in this work was higher than cellulose[81], alginate[82], dextran[83] and gelatin methacryloyl[84], which were often applied in commercial wound dressings. The results on DN hydrogels was also comparable to the dry chitin based dressings with excellent fibroblast proliferation promotion effect[85, 86]. At the similar water content, the accelerated effect of the DN hydrogel was better than that of the crosslinked PEG hydrogel, collagen/alginate/cellulose composite hydrogel and glucomannan/PNVP composite hydrogel[87-89]. After day 3, cells contacting with hydrogels showed steady increase while cells on petri dish showed acceleration. The result suggested that cells on petri dish just proceeded from lag phase to log phase at day 3 while cells on hydrogel were stimulated to grow quickly from the very beginning. Lag phase meant the slow proliferation phase at beginning that cells need to adapt the growth environment and adsorb

nutrients for adhesion, transformation and then proliferation, normally it would take days, and after the lag phase it was the log phase for explosive growth. It was clear to see that the cells increased fastest on the DN hydrogel, which indicated the most effective stimulation on fibroblasts, suggesting an accelerating fibroblast proliferation during wound healing.

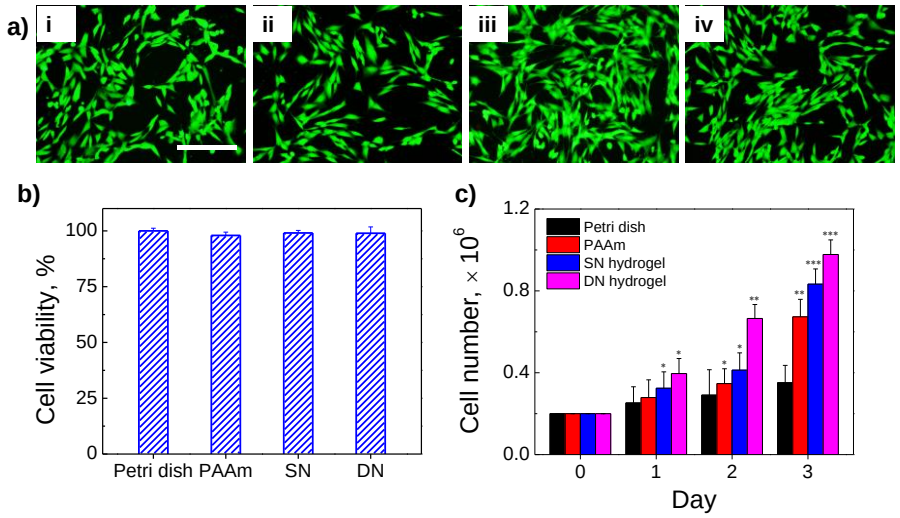

Figure 4. (a) Fluorescent microscope images of living cells stained with Calcein-AM (green), and dead cells stained with PI (red) after incubation on the petri dish (i), PAAm hydrogel (ii), SN hydrogel (iii) and DN hydrogel (iv) for 24 h. (Scale bar = 200 μm) (b) Cell viability of NIH3T3 cells after incubation on the samples for 24 h. (c) Proliferation of NIH3T3 cells on the petri dish and under the PAAm, SN and DN hydrogel. Each measurement was performed in triplicate. Statistical significance ($^{*}p < 0.05$, $^{**}p < 0.01$ and $^{***}p < 0.001$) between the hydrogel sample and blank control was analyzed using the one-way ANOVA test by SPSS Statistical software.

As a potential repairing material, the direct contact of the DN hydrogel with the superficial soft tissues was necessary, hence the importance of its biosafety should be concerned. To examine the biosafety of the DN hydrogel *in vivo*, a subcutaneous implantation surgery was employed on

rabbits, which presented similarities to humans with respect to fracture resistance[90, 91]. The DN hydrogel was implanted under the dorsal skin of a rabbit through an incision (**Figure 5a**). Due to non-adhesion of the DN hydrogel to body tissue, surgical suture was necessary for hydrogel immobilization (Figure 5b-i). Generally, an injured tissue would take weeks to recover, and herein, the implantation was allowed to perform for weeks to examine the inflammation response *in vivo*. After 1, 2 and 4 weeks, the implanted hydrogel was resected for subsequent pathological examination. As shown in Figure 5b-ii, the vessels macroscopically grew surrounding the hydrogel without abnormal findings. Further, the pathologic specimens were obtained from both control and the hydrogel-contacted tissues after 1, 2 and 4 weeks and H&E staining was performed (Figure 5c). At the first week, it was clear to find out fibroblasts and collagen fibers upon the stratum granulosum. And the number of fibroblasts and collagen fibers generated much more when the tissue was contact with the hydrogel. At the second week, the tissue layer upon the stratum granulosum grew thicker, and thickness of the new generated tissue (green dashed line) contacted with hydrogel was larger than that without hydrogel contact, suggesting a faster tissue healing under the effect of DN hydrogel. At the fourth week, both the tissue layer upon the stratum granulosum with and without hydrogel contact became thinner than that appeared at the second week and suggested the late stage of wound healing involving degradation of collagen fibers. During this healing process, it was rare to find any inflammatory cells, *e.g.* neutrophils, macrophages and lymphocytes, which demonstrated almost no inflammation was induced by the foreign DN hydrogel, suggesting the good biosafety to the body tissues *in vivo*.

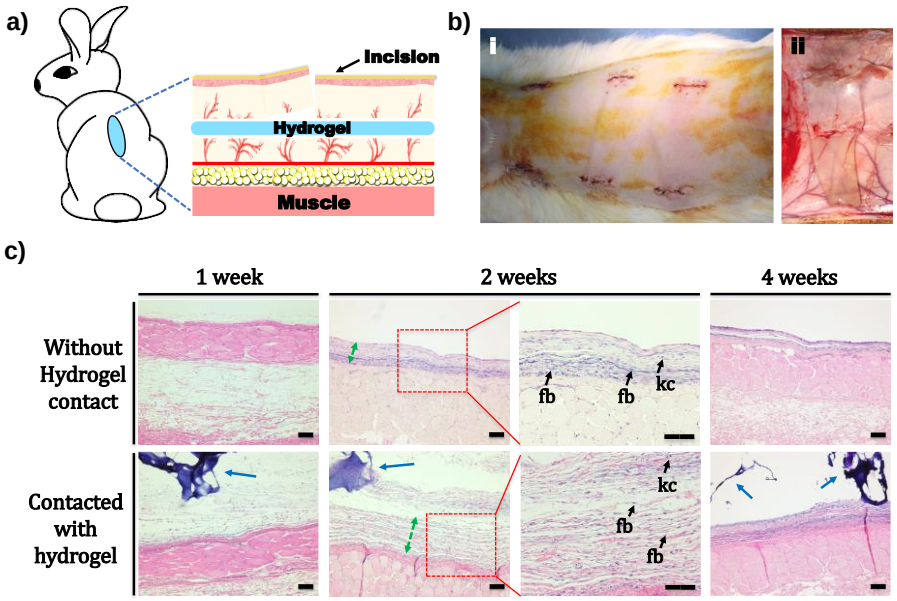

505

506 **Figure 5.** (a) Scheme of the *in vivo* implanted hydrogel. (b) Photographs of the rabbit dorsum at 1
507 week after implantation (i) and the implanted hydrogel (ii). (c) Histopathologic profiles of the
508 tissues without and with hydrogel contact. Hematoxylin and eosin (H&E) staining was used for
509 the examination. The black arrowed showed the fibroblasts (fb) and keratinocytes (kc) at the
510 second week. The blue arrows indicate the pieces of DN hydrogel. (Scale bar = 100 μm).

511

512 **Conclusion**

513 In this work, we prepared a biosafe DN hydrogel composed of hybrid RCNs-PEGDE as the first
514 network and PAAm as the second network. The DN strategy significant enhanced the mechanical
515 properties of RCNs hydrogel and reserved the ability of bacterial resistant and fibroblast
516 proliferation from chitin. Also, from the animal experiments the DN hydrogel was proved to be
517 biosafe. These properties of chitin based DN hydrogel would realize its full potential as
518 regenerative materials using for wound healing and even grafting applications. Also, the idea that

applying a hybrid network composed of stiff nanofibers and flexible co-polymer to prepare the DN hydrogels would inspire others to find out a different approach for natural polymer applications. Future chitin based DN hydrogel development considering *in vivo* degradation may broaden the applications in clinical therapeutic fields.

Acknowledgments

This work was supported by JSPS KAKENHI (Grant Numbers JP17H06144). Institute for Chemical Reaction Design and Discovery (WPI-ICReDD) was established by World Premier International Research Initiative (WPI), MEXT, Japan.

References

1. Kamoun, E. A.; Kenawy, E. R. S.; Chen, X., A review on polymeric hydrogel membranes for wound dressing applications: PVA-based hydrogel dressings. *J. Adv. Res.*, **2017**, 8(3), 217-233.
2. Mir, M.; Ali, M. N.; Barakullah, A.; Gulzar, A.; Arshad, M.; Fatima, S.; Asad, M., Synthetic polymeric biomaterials for wound healing: a review. *Prog. Biomater.*, **2018**, 7(1), 1-21.
3. Jones, A.; Vaughan, D., Hydrogel dressings in the management of a variety of wound types: A review. *Orthop. Nurs.*, **2005**, 9, S1-S11.
4. Zhao, W.; Jin, X.; Cong, Y.; Liu, Y. Y.; Fu, J., Degradable natural polymer hydrogels for articular cartilage tissue engineering. *J. Chem. Technol. Biotechnol.*, **2013**, 88(3), 327-339.
5. Pina, S.; Oliveira, J. M.; Reis, R. L., Natural-based nanocomposites for bone tissue engineering and regenerative medicine: A review. *Adv. Mater.*, **2015**, 27(7), 1143-1169.
6. Matthew, I. R.; Browne, R. M.; Frame, J. W.; Millar, B. G., Subperiosteal Behavior of Alginate and Cellulose Wound Dressing Materials. *Biomaterials*, **1995**, 16(4), 275-278.
7. Lee, K. Y.; Mooney, D. J., Alginate: Properties and biomedical applications. *Prog. Polym. Sci.*, **2012**, 37(1), 106-126.
8. Helary, C.; Abed, A.; Mosser, G.; Louedec, L.; Letourneur, D.; Coradin, T.; Giraud-Guille, M. M.; Meddahi-Pelle, A., Evaluation of dense collagen matrices as medicated wound dressing for the treatment of cutaneous chronic wounds. *Biomater. Sci.*, **2015**, 3(2), 373-382.
9. Sun, G. M.; Zhang, X. J.; Shen, Y. I.; Sebastian, R.; Dickinson, L. E.; Fox-Talbot, K.; Reinblatt, M.; Steenbergen, C.; Harmon, J. W.; Gerecht, S., Dextran hydrogel scaffolds enhance angiogenic responses and promote complete skin regeneration during burn wound healing. *Proc. Natl. Acad. Sci. U.S.A.*, **2011**, 108(52), 20976-20981.
10. Vepari, C.; Kaplan, D. L., Silk as a biomaterial. *Prog. Polym. Sci.*, **2007**, 32(8-9), 991-1007.

11. Ghosh, K.; Ren, X. D.; Shu, X. Z.; Prestwich, G. D.; Clark, R. A. F., Fibronectin functional domains coupled to hyaluronan stimulate adult human dermal fibroblast responses critical for wound healing. *Tissue Eng.*, **2006**, 12(3), 601-613.
12. Zhao, X.; Wu, H.; Guo, B. L.; Dong, R. N.; Qiu, Y. S.; Ma, P. X., Antibacterial anti-oxidant electroactive injectable hydrogel as self-healing wound dressing with hemostasis and adhesiveness for cutaneous wound healing. *Biomaterials*, **2017**, 122, 34-47.
13. Singh, B.; Sharma, S.; Dhiman, A., Design of antibiotic containing hydrogel wound dressings: Biomedical properties and histological study of wound healing. *Int. J. Pharm.*, **2013**, 457(1), 82-91.
14. Wang, Y. F.; Li, P. F.; Xiang, P.; Lu, J. T.; Yuan, J.; Shen, J., Electrospun polyurethane/keratin/AgNP biocomposite mats for biocompatible and antibacterial wound dressings. *J. Mater. Chem. B*, **2016**, 4(4), 635-648.
15. Shalumon, K. T.; Anulekha, K. H.; Nair, S. V.; Nair, S. V.; Chennazhi, K. P.; Jayakumar, R., Sodium alginate/poly(vinyl alcohol)/nano ZnO composite nanofibers for antibacterial wound dressings. *Int. J. Biol. Macromol.*, **2011**, 49(3), 247-254.
16. Padmanabhan, J.; Kyriakides, T. R., Nanomaterials, Inflammation, and Tissue Engineering. *Wiley Interdiscip. Rev.: Nanomed. Nanobiotechnol.*, **2015**, 7(3), 355-370.
17. Di Felice, G.; Colombo, P., Nanoparticle–allergen complexes for allergen immunotherapy. *Int. J. Nanomed.*, **2017**, 12, 4493-4504.
18. Jayakumar, R.; Prabaharan, M.; Kumar, P. T. S.; Nair, S. V.; Tamura, H., Biomaterials based on chitin and chitosan in wound dressing applications. *Biotechnol. Adv.*, **2011**, 29(3), 322-337.
19. Prashanth, K. V. H.; Tharanathan, R. N., Chitin/chitosan: modifications and their unlimited application potential - an overview. *Trends Food Sci. Technol.*, **2007**, 18(3), 117-131.
20. Ohshima, Y.; Nishino, K.; Yonekura, Y.; Kishimoto, S.; Wakabayashi, S., Clinical application of chitin non-woven fabric as wound dressing. *Eur. J. Plast. Surg.*, **1987**, 10(2), 66-69.
21. Watthanaphanit, A.; Supaphol, P.; Tamura, H.; Tokura, S.; Rujiravanit, R., Fabrication, structure, and properties of chitin whisker-reinforced alginate nanocomposite fibers. *J. Appl. Polym. Sci.*, **2008**, 110(2), 890-899.
22. Jayakumar, R.; Prabaharan, M.; Nair, S. V.; Tamura, H., Novel chitin and chitosan nanofibers in biomedical applications. *Biotechnol. Adv.*, **2010**, 28(1), 142-150.
23. Discher, D. E.; Janmey, P.; Wang, Y. L., Tissue cells feel and respond to the stiffness of their substrate. *Science*, **2005**, 310(5751), 1139-1143.
24. Kloxin, A. M.; Benton, J. A.; Anseth, K. S., *In situ* elasticity modulation with dynamic substrates to direct cell phenotype. *Biomaterials*, **2010**, 31(1), 1-8.
25. Missirlis, D.; Spatz, J. P., Combined Effects of PEG Hydrogel Elasticity and Cell-Adhesive Coating on Fibroblast Adhesion and Persistent Migration. *Biomacromolecules*, **2014**, 15(1), 195-205.
26. Wang, H.; Tibbitt, M. W.; Langer, S. J.; Leinwand, L. A.; Anseth, K. S., Hydrogels preserve native phenotypes of valvular fibroblasts through an elasticity-regulated PI3K/AKT pathway. *Proc. Natl. Acad. Sci. U.S.A.*, **2013**, 110(48), 19336-19341.
27. Webb, K.; Li, W. H.; Hitchcock, R. W.; Smeal, R. M.; Gray, S. D.; Tresco, P. A., Comparison of human fibroblast ECM-related gene expression on elastic three-dimensional substrates relative to two-dimensional films of the same material. *Biomaterials*, **2003**, 24(25), 4681-4690.
28. Yu, P.; Xie, J.; Chen, Y.; Liu, J. M.; Liu, Y. P.; Bi, B.; Luo, J.; Li, S. Y.; Jiang, X. L.; Li, J. S., A thermo-sensitive injectable hydroxypropyl chitin hydrogel for sustained salmon calcitonin release with enhanced osteogenesis and hypocalcemic effects. *J. Mater. Chem. B*, **2020**, 8(2), 270-281.
29. Liu, H.; Liu, J.; Qi, C.; Fang, Y. P.; Zhang, L. N.; Zhuo, R. X.; Jiang, X. L., Thermosensitive injectable in-situ forming carboxymethyl chitin hydrogel for three-dimensional cell culture. *Acta Biomater.*, **2016**, 35, 228-237.
30. Bi, B.; Liu, H.; Kang, W. T.; Zhuo, R. X.; Jiang, X. L., An injectable enzymatically crosslinked tyramine-modified carboxymethyl chitin hydrogel for biomedical applications. *Colloids Surf., B*, **2019**, 175, 614-624.
31. Ifuku, S.; Saimoto, H., Chitin nanofibers: preparations, modifications, and applications. *Nanoscale*, **2012**, 4(11), 3308-3318.
32. Nawawi, W. M. F. W.; Lee, K. Y.; Kontturi, E.; Murphy, R. J.; Bismarck, A., Chitin Nanopaper from Mushroom Extract: Natural Composite of Nanofibers and Glucan from a Single Biobased Source. *ACS Sustain. Chem. Eng.*, **2019**, 7(7), 6492-6496.

33. Jin, J.; Lee, D.; Im, H. G.; Han, Y. C.; Jeong, E. G.; Rolandi, M.; Choi, K. C.; Bae, B. S., Chitin Nanofiber Transparent Paper for Flexible Green Electronics. *Adv. Mater.*, **2016**, 28(26), 5169-5175.
34. Kim, K.; Ha, M.; Choi, B.; Joo, S. H.; Kang, H. S.; Park, J. H.; Gu, B.; Park, C.; Park, C.; Kim, J.; Kwak, S. K.; Ko, H.; Jin, J.; Kang, S. J., Biodegradable, electro-active chitin nanofiber films for flexible piezoelectric transducers. *Nano Energy*, **2018**, 48, 275-283.
35. Shou, K. Q.; Huang, Y.; Qi, B. W.; Hu, X.; Ma, Z. J.; Lu, A.; Jian, C.; Zhang, L. N.; Yu, A. X., Induction of mesenchymal stem cell differentiation in the absence of soluble inducer for cutaneous wound regeneration by a chitin nanofiber-based hydrogel. *J. Tissue Eng. Regen. Med.*, **2018**, 12(2), E867-E880.
36. Chen, C. C.; Yano, H.; Li, D. G.; Abe, K., Preparation of high-strength α-chitin nanofiber-based hydrogels under mild conditions. *Cellulose*, **2015**, 22(4), 2543-2550.
37. Zhong, C.; Cooper, A.; Kapetanovic, A.; Fang, Z. H.; Zhang, M. Q.; Rolandi, M., A facile bottom-up route to self-assembled biogenic chitin nanofibers. *Soft Matter*, **2010**, 6(21), 5298-5301.
38. Fang, Y.; Duan, B.; Lu, A.; Liu, M. L.; Liu, H. L.; Xu, X. J.; Zhang, L. N., Intermolecular Interaction and the Extended Wormlike Chain Conformation of Chitin in NaOH/Urea Aqueous Solution. *Biomacromolecules*, **2015**, 16(4), 1410-1417.
39. Rolandi, M.; Rolandi, R., Self-assembled chitin nanofibers and applications. *Adv. Colloid Interface Sci.*, **2014**, 207, 216-222.
40. Bai, L.; Huan, S. Q.; Xiang, W. C.; Liu, L.; Yang, Y.; Nugroho, R. W. N.; Fan, Y. M.; Rojas, O. J., Self-Assembled Networks of Short and Long Chitin Nanoparticles for Oil/Water Interfacial Superstabilization. *ACS Sustain. Chem. Eng.*, **2019**, 7(7), 6497-6511.
41. Cortizo, M. S.; Berghoff, C. F.; Alessandrini, J. L., Characterization of chitin from Illex argentinus squid pen. *Carbohydr. Polym.*, **2008**, 74(1), 10-15.
42. Li, G. X.; Du, Y. M.; Tao, Y. Z.; Liu, Y. T.; Li, S.; Hu, X. W.; Yang, J. H., Dilute solution properties of four natural chitin in NaOH/urea aqueous system. *Carbohydr. Polym.*, **2010**, 80(3), 970-976.
43. Gong, J. P.; Katsuyama, Y.; Kurokawa, T.; Osada, Y., Double-network hydrogels with extremely high mechanical strength. *Adv. Mater.*, **2003**, 15(14), 1155-1158.
44. Gong, J. P., Why are double network hydrogels so tough? *Soft Matter*, **2010**, 6(12), 2583-2590.
45. Nakajima, T.; Ozaki, Y.; Namba, R.; Ota, K.; Maida, Y.; Matsuda, T.; Kurokawa, T.; Gong, J. P., Tough Double-Network Gels and Elastomers from the Nonprestretched First Network. *ACS Macro Lett.*, **2019**, 8(11), 1407-1412.
46. Wang, J.; Yuan, B.; Han, R. P. S., Modulus of elasticity of randomly and aligned polymeric scaffolds with fiber size dependency. *J. Mech. Behav. Biomed. Mater.*, **2018**, 77, 314-320.
47. He, M.; Wang, Z. G.; Cao, Y.; Zhao, Y. T.; Duan, B.; Chen, Y.; Xu, M.; Zhang, L. N., Construction of Chitin/PVA Composite Hydrogels with Jellyfish Gel-Like Structure and Their Biocompatibility. *Biomacromolecules*, **2014**, 15(9), 3358-3365.
48. Chang, C.; Peng, N.; He, M.; Teramoto, Y.; Nishio, Y.; Zhang, L., Fabrication and properties of chitin/hydroxyapatite hybrid hydrogels as scaffold nano-materials. *Carbohydr. Polym.*, **2013**, 91(1), 7-13.
49. Chang, C. Y.; Chen, S.; Zhang, L. N., Novel hydrogels prepared via direct dissolution of chitin at low temperature: structure and biocompatibility. *J. Mater. Chem.*, **2011**, 21(11), 3865-3871.
50. Huang, J.; Zhong, Y.; Zhang, L.; Cai, J., Extremely Strong and Transparent Chitin Films: A High-Efficiency, Energy-Saving, and "Green" Route Using an Aqueous KOH/Urea Solution. *Adv. Funct. Mater.*, **2017**, 27(26), 1701100.
51. Poirier, M.; Charlet, G., Chitin fractionation and characterization in N,N-dimethylacetamide/lithium chloride solvent system. *Carbohydr. Polym.*, **2002**, 50(4), 363-370.
52. Raymond, L.; Morin, F. G.; Marchessault, R. H., Degree of Deacetylation of Chitosan Using Conductometric Titration and Solid-State Nmr. *Carbohydr. Res.*, **1993**, 246, 331-336.
53. Ding, B.; Zhao, D.; Song, J.; Gao, H.; Xu, D.; Xu, M.; Cao, X.; Zhang, L.; Cai, J., Light weight, mechanically strong and biocompatible α-chitin aerogels from different aqueous alkali hydroxide/urea solutions. *Sci. China: Chem.*, **2016**, 59(11), 1405-1414.
54. Salick, D. A.; Kretsinger, J. K.; Pochan, D. J.; Schneider, J. P., Inherent antibacterial activity of a peptide-based β-hairpin hydrogel. *J. Am. Chem. Soc.*, **2007**, 129(47), 14793-14799.
55. Nagahama, H.; Higuchi, T.; Jayakumar, R.; Furuike, T.; Tamura, H., XRD studies of β-chitin from squid pen with calcium solvent. *Int. J. Biol. Macromol.*, **2008**, 42(4), 309-313.

56. Nakajima, T.; Kurokawa, T.; Ahmed, S.; Wu, W. L.; Gong, J. P., Characterization of internal fracture process of double network hydrogels under uniaxial elongation. *Soft Matter*, **2013**, 9(6), 1955-1966.
57. Liu, M. X.; Huang, J. D.; Luo, B. H.; Zhou, C. R., Tough and highly stretchable polyacrylamide nanocomposite hydrogels with chitin nanocrystals. *Int. J. Biol. Macromol.*, **2015**, 78, 23-31.
58. Huang, Y.; Yao, M. Y.; Zheng, X.; Liang, X. C.; Su, X. J.; Zhang, Y.; Lu, A.; Zhang, L. N., Effects of Chitin Whiskers on Physical Properties and Osteoblast Culture of Alginate Based Nanocomposite Hydrogels. *Biomacromolecules*, **2015**, 16(11), 3499-3507.
59. Ramos, M. L. P.; Gonzalez, J. A.; Albornoz, S. G.; Perez, C. J.; Villanueva, M. E.; Giorgieri, S. A.; Copello, G. J., Chitin hydrogel reinforced with TiO_2 nanoparticles as an arsenic sorbent. *Chem. Eng. J.*, **2016**, 285, 581-587.
60. Liu, M. X.; Zhang, Y.; Li, J. J.; Zhou, C. R., Chitin-natural clay nanotubes hybrid hydrogel. *Int. J. Biol. Macromol.*, **2013**, 58, 23-30.
61. Xu, D.; Huang, J.; Zhao, D.; Ding, B.; Zhang, L.; Cai, J., High-flexibility, high-toughness double-cross-linked chitin hydrogels by sequential chemical and physical cross-linkings. *Adv. Mater.*, **2016**, 28(28), 5844-5849.
62. Abe, K.; Ifuku, S.; Kawata, M.; Yano, H., Preparation of tough hydrogels based on β-chitin nanofibers via NaOH treatment. *Cellulose*, **2014**, 21(1), 535-540.
63. Chen, C. C.; Li, D. G.; Yano, H.; Abe, K., Bioinspired hydrogels: Quinone crosslinking reaction for chitin nanofibers with enhanced mechanical strength via surface deacetylation. *Carbohydr. Polym.*, **2019**, 207, 411-417.
64. Liu, L.; Wang, R.; Yu, J.; Jiang, J.; Zheng, K.; Hu, L. J.; Wang, Z. G.; Fan, Y. M., Robust Self-Standing Chitin Nanofiber/Nanowhisker Hydrogels with Designed Surface Charges and Ultralow Mass Content via Gas Phase Coagulation. *Biomacromolecules*, **2016**, 17(11), 3773-3781.
65. Mushi, N. E.; Kochumalayil, J.; Cervin, N. T.; Zhou, Q.; Berglund, L. A., Nanostructurally Controlled Hydrogel Based on Small-Diameter Native Chitin Nanofibers: Preparation, Structure, and Properties. *Chemsuschem*, **2016**, 9(9), 989-995.
66. Oh, D. X.; Kim, S.; Lee, D.; Hwang, D. S., Tunicate-mimetic nanofibrous hydrogel adhesive with improved wet adhesion. *Acta Biomater.*, **2015**, 20, 104-112.
67. Santos, A.; Lagares, D., Matrix Stiffness: the Conductor of Organ Fibrosis. *Curr. Rheumatol. Rep.*, **2018**, 20(1), 2.
68. Es-haghi, S. S.; Weiss, R. A., Fabrication of Tough Hydrogels from Chemically Cross-Linked Multiple Neutral Networks. *Macromolecules*, **2016**, 49(23), 8980-8987.
69. Benhabiles, S.; Salah, R.; Lounici, H.; Drouiche, N.; Goosen, M. F. A.; Mameri, N., Antibacterial activity of chitin, chitosan and its oligomers prepared from shrimp shell waste. *Food Hydrocolloids*, **2012**, 29(1), 48-56.
70. Huang, J.; Zhong, Y.; Zhang, L.; Cai, J., Distinctive Viewpoint on the Rapid Dissolution Mechanism of α-Chitin in Aqueous Potassium Hydroxide–Urea Solution at Low Temperatures. *Macromolecules*, **2020**, 53(13), 5588-5598.
71. Balouiri, M.; Sadiki, M.; Ibnsouda, S. K., Methods for in vitro evaluating antimicrobial activity: A review. *J. Pharm. Anal.*, **2016**, 6(2), 71-79.
72. Frauenlob, M.; King, D. R.; Guo, H. L.; Ishihara, S.; Tsuda, M.; Kurokawa, T.; Haga, H.; Tanaka, S.; Gong, J. P., Modulation and Characterization of the Double Network Hydrogel Surface-Bulk Transition. *Macromolecules*, **2019**, 52(17), 6704-6713.
73. Rabea, E. I.; Badawy, M. E. T.; Stevens, C. V.; Smagghe, G.; Steurbaut, W., Chitosan as antimicrobial agent: Applications and mode of action. *Biomacromolecules*, **2003**, 4(6), 1457-1465.
74. Yuki Shibata; Takayuki Kurokawa; Tomoyasu Aizawa; Gong, J. P., Bactericidal effect of cationic hydrogels prepared from hydrophilic polymers. *J. Appl. Polym. Sci.*, **2020**, e49583.
75. Huang, Y. C.; Vieira, A.; Huang, K. L.; Yeh, M. K.; Chiang, C. H., Pulmonary inflammation caused by chitosan microparticles. *J. Biomed. Mater. Res. A*, **2005**, 75A(2), 283-287.
76. Drury, J. L.; Mooney, D. J., Hydrogels for tissue engineering: scaffold design variables and applications. *Biomaterials*, **2003**, 24(24), 4337-4351.
77. Mori, T.; Okumura, M.; Matsuura, M.; Ueno, K.; Tokura, S.; Okamoto, Y.; Minami, S.; Fujinaga, T., Effects of chitin and its derivatives on the proliferation and cytokine production of fibroblasts in vitro. *Biomaterials*, **1997**, 18(13), 947-951.
78. Chatelet, C.; Damour, O.; Domard, A., Influence of the degree of acetylation on some biological properties of chitosan films. *Biomaterials*, **2001**, 22(3), 261-268.

79. Roehm, N. W.; Rodgers, G. H.; Hatfield, S. M.; Glasebrook, A. L., An improved colorimetric assay for cell proliferation and viability utilizing the tetrazolium salt XTT. *J. Immunol. Methods*, **1991**, 142(2), 257-265.
80. Howling, G. I.; Dettmar, P. W.; Goddard, P. A.; Hampson, F. C.; Dornish, M.; Wood, E. J., The effect of chitin and chitosan on the proliferation of human skin fibroblasts and keratinocytes in vitro. *Biomaterials*, **2001**, 22(22), 2959-2966.
81. Lin, S.-P.; Kung, H.-N.; Tsai, Y.-S.; Tseng, T.-N.; Hsu, K.-D.; Cheng, K.-C., Novel dextran modified bacterial cellulose hydrogel accelerating cutaneous wound healing. *Cellulose*, **2017**, 24(11), 4927-4937.
82. des Rieux, A.; De Berdt, P.; Ansorena, E.; Ucakar, B.; Damien, J.; Schakman, O.; Audouard, E.; Bouzin, C.; Auhl, D.; Simon-Yarza, T.; Feron, O.; Blanco-Prieto, M. J.; Carmeliet, P.; Bailly, C.; Clotman, F.; Preat, V., Vascular endothelial growth factor-loaded injectable hydrogel enhances plasticity in the injured spinal cord. *J. Biomed. Mater. Res. A*, **2014**, 102(7), 2345-2355.
83. Wang, Z.; Zhu, X.; Zhang, R., Characterization and Analysis of Collective Cellular Behaviors in 3D Dextran Hydrogels with Homogenous and Clustered RGD Compositions. *Materials*, **2019**, 12(20), 3391.
84. Yoon, H. J.; Shin, S. R.; Cha, J. M.; Lee, S. H.; Kim, J. H.; Do, J. T.; Song, H.; Bae, H., Cold Water Fish Gelatin Methacryloyl Hydrogel for Tissue Engineering Application. *PLoS One*, **2016**, 11(10), e0163902.
85. Murakami, K.; Aoki, H.; Nakamura, S.; Nakamura, S.; Takikawa, M.; Hanzawa, M.; Kishimoto, S.; Hattori, H.; Tanaka, Y.; Kiyosawa, T.; Sato, Y.; Ishihara, M., Hydrogel blends of chitin/chitosan, fucoidan and alginate as healing-impaired wound dressings. *Biomaterials*, **2010**, 31(1), 83-90.
86. Abdel-Mohsen, A. M.; Jancar, J.; Massoud, D.; Fohlerova, Z.; Elhadidy, H.; Spotz, Z.; Hebeish, A., Novel chitin/chitosan-glucan wound dressing: Isolation, characterization, antibacterial activity and wound healing properties. *Int. J. Pharm.*, **2016**, 510(1), 86-99.
87. Kumar, A.; Wang, X.; Nune, K. C.; Misra, R. D. K., Biodegradable hydrogel-based biomaterials with high absorbent properties for non-adherent wound dressing. *Int. Wound J.*, **2017**, 14(6), 1076-1087.
88. Shahbuddin, M.; Bullock, A. J.; MacNeil, S.; Rimmer, S., Glucomannan-poly(N-vinyl pyrrolidinone) bicomponent hydrogels for wound healing. *J. Mater. Chem. B*, **2014**, 2(6), 727-738.
89. Watanabe, J.; Ooya, T.; Nitta, K. H.; Park, K. D.; Kim, Y. H.; Yui, N., Fibroblast adhesion and proliferation on poly(ethylene glycol) hydrogels crosslinked by hydrolyzable polyrotaxane. *Biomaterials*, **2002**, 23(20), 4041-4048.
90. Calasans-Maia, M. D.; Monteiro, M. L.; Ascoli, F. O.; Granjeiro, J. M., The rabbit as an animal model for experimental surgery. *Acta Cir. Bras.*, **2009**, 24(4), 325-328.
91. Valiense, H.; Barreto, M.; Resende, R. F.; Alves, A. T.; Rossi, A. M.; Mavropoulos, E.; Granjeiro, J. M.; Calasans-Maia, M. D., In vitro and in vivo evaluation of strontium-containing nanostructured carbonated hydroxyapatite/sodium alginate for sinus lift in rabbits. *J. Biomed. Mater. Res. B*, **2016**, 104(2), 274-282.

Supporting information

Table of Contents

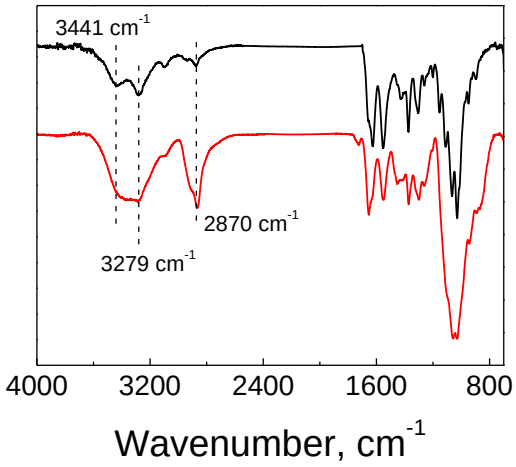

Figure S1. ATR-FTIR result of β-chitin (black) and SN hydrogel (red) in the dry state. The wavenumber of 2870 cm^{-1} was assigned to the stretching vibration of -CH_2- group, and the wavenumber of 3279 and 3441 cm^{-1} were assigned to the stretching vibration of -OH group on SN network, respectively.

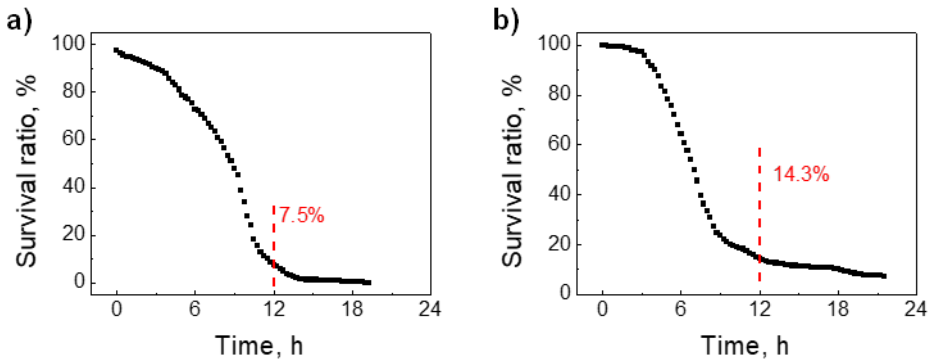

Figure S2. Time evolution of survival ratio of *M. luteus* (a) and *E. coli* (b) incubated on the SN hydrogel.

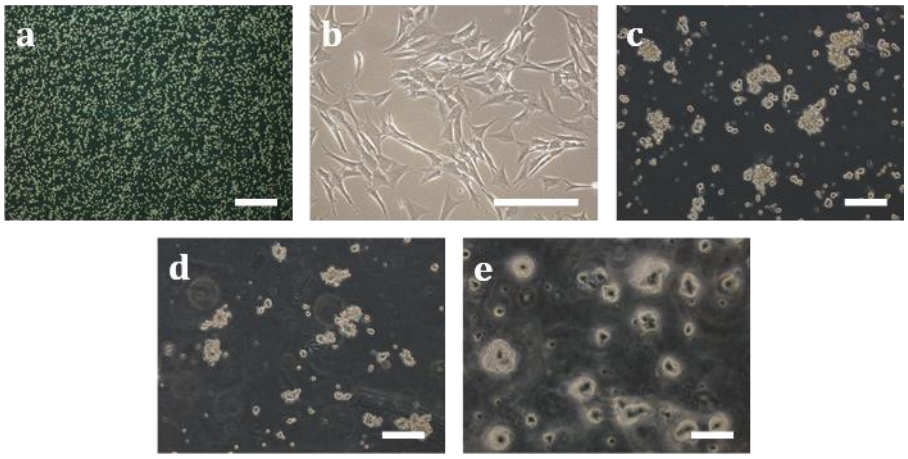

Figure S3. Photographs of NIH-3T3 cells suspension (a) and after cultivation on the petri dish (b), PAAm (c), SN (d) and DN (e) hydrogels. Scale bar = 200 μm.

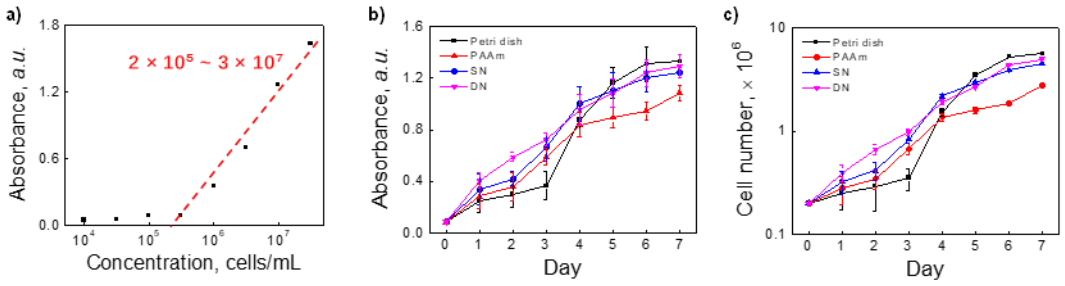

Figure S4. (a) Calibration curve of absorbance versus cell concentration. The linear area is between 3×10^5 to 3×10^7 cells·mL^{-1} (SD ≈ 5.8%). (b, c) The time evolutions of absorbance (b) and the calculated cell numbers (c) for cells incubated on petri dish and between petri dish and each hydrogel sample.

Table S1. The relative swelling ratio of the DN hydrogel in various solutions in relative to that in pure water.

Solutions	Relative swelling ratio [a]
Physiological Saline (pH=7.0)	0.86
PBS buffer (pH=7.4)	0.81
pH=5.0 [b]	0.92
pH=10.0 [b]	0.89

[a] The relative swelling ratio was calculated according to the volume ratio between the samples in ionic solutions and that in water.

[b] The pH value of the solutions were only adjust by 0.1 mol/L HCl and NaOH solution, respectively.

Movie S1. Time-dependent bacteria killing test of *M. luteus* and *E. coli* on SN hydrogel. Each snapshot was taken every 15 minutes by a fluorescent microscope with time-lapse system (Eclipse Ti-E Inverted Microscope, Nikon Instruments Inc., Japan) then aligned into an animation by the accessory software.

For Table of Contents use only

Chitin-based double-network hydrogel as potential superficial soft tissue repairing materials

Junchao Huang, [a] Martin Frauenlob, [a] Yuki Shibata, [a] Lei Wang, [b, c] Tasuku Nakajima, [a, c, d] Takayuki Nonoyama, [a, c] Masumi Tsuda, [b, c, d] Shinya Tanaka, [b, c, d] Takayuki Kurokawa, [a, c] Jian Ping Gong [a, c, d,*]